

# The Conformational Analysis of Three Derivatives of Erythromycin A: (9*S*)-9-Hydroxy-9-deoxyerythromycin A, (9*S*)-9,11-*O*-Isopropylidene-9-deoxyerythromycin A, and (9*S*)-Erythromycylamine A by Nuclear Magnetic Resonance Spectroscopy and Molecular Modelling

Jeremy R. Everett\* and John W. Tyler

Beecham Pharmaceuticals, Brockham Park, Betchworth, Surrey, RH3 7AJ

The  $^1\text{H}$  and  $^{13}\text{C}$  n.m.r. spectra of (9*S*)-9-hydroxy-9-deoxyerythromycin A (2), (9*S*)-9, 11-*O*-isopropylidene-9-deoxyerythromycin A (3), and (9*S*)-erythromycylamine A (4) were solved by two-dimensional (2D) n.m.r. methods. The solution conformations of compounds (2), (3), and (4) were then determined by n.m.r. spectroscopy [n.O.e.(1D and 2D) and  $T_1$  experiments] and compared with the solution conformation of erythromycin A (1). In each case the cladinose and desosamine sugars are in the same chair conformations as found in (1). Furthermore the overall orientations of both sugars were found to be very similar to those of (1) in all cases. However, the lactone rings of (2) and (4) were found to be in fast exchange between conformations characterised as 'folded-in' or 'folded-out' in the C-3 to C-5 region, whereas the lactone ring of (3) was predominantly in a 'folded-out' conformation, as was found for (1). The 'folded-in' conformations are novel and have not been previously described. Molecular modelling was used in order to compare the solution-state conformations with crystalline-state models of the two types of lactone ring conformation. No simple correlation was found between the solution-state conformational preferences of compounds (1)–(4) and their antibacterial activities.

Erythromycin A (1) is a medically important macrolide antibiotic composed of a polyfunctionalised 14-membered lactone ring substituted with desosamine and cladinose sugar units. The solution conformations of (1) and the motional properties of its methyl groups and sugar rings have been studied recently by  $^1\text{H}$  and  $^{13}\text{C}$  n.m.r. spectroscopy.<sup>1</sup> The logical progression of this work was to study derivatives of (1) with differing antibacterial activities. A preliminary communication on compounds (1) and (2) has appeared.<sup>2</sup> This paper describes the results of a study on compounds (2),<sup>2-4</sup> (3),<sup>5</sup> and (4).<sup>6</sup> This study had five main aims.

(i) the analysis of the  $^1\text{H}$  and  $^{13}\text{C}$  n.m.r. spectra of compounds (2), (3), and (4).

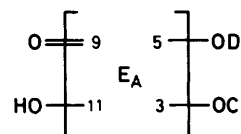
(ii) the determination of the solution conformations of compounds (2), (3), and (4).

(iii) the determination of the motional properties of the methyl groups and the sugar rings of compounds (2), (3), and (4) in solution.

(iv) the comparison of the solution conformations and motional properties of compounds (2), (3), and (4) with both the crystalline-state conformations of erythromycin A hydroiodide dihydrate and (5) and the motional properties predicted for these crystal structures.

(v) the determination of possible correlations between the antibacterial activities of compounds (1)–(4) and their solution-state conformations.

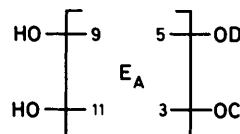
The structure of erythromycin A ( $E_A$ ) (1) may be represented as



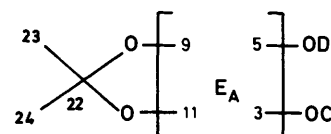
D = Desosamine

C = Cladinose

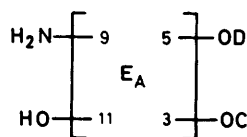
The structures of (9*S*)-9-hydroxy-9-deoxyerythromycin A (2), (9*S*)-9,11-*O*-isopropylidene-9-deoxyerythromycin A (3), (9*S*)-erythromycylamine A (4), and (9*S*)-9-*N*, 11-*O*-[2-(2-methoxyethoxy)ethylidene]erythromycylamine A (5) are given below using the same representation.



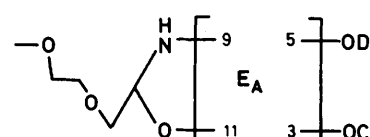
(2)



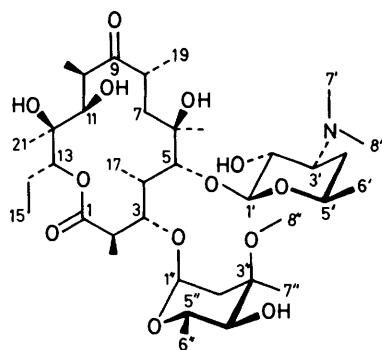
(3)



(4)



(5)



(1) †

† This new representation of (1) is preferred over our previous conventional drawings since (i) the lactone moiety is correctly drawn *trans*, (ii) the major conformations are explicit, and (iii) the problems of defining stereochemistry at 'inside-corner' carbons are eliminated. We thank Dr W. D. Celmer for helpful advice on this matter.

**Table 1.**  $^1\text{H}$  N.m.r. chemical shifts ( $\delta_{\text{H}}$  in p.p.m.) for (1)–(4) in  $\text{CDCl}_3$ – $\text{Me}_4\text{Si}$ 

Proton	(1) <sup>7</sup>	(2)	(3)	(4)
1	—	—	—	—
2	2.87	2.74	2.90	2.74
3	3.99	4.09	4.21	4.11
4	1.97	1.88	2.01	1.89
5	3.56	3.68	3.63	3.71
6	—	—	—	—
7	1.93, 1.74	1.64, 1.29	1.75, 1.46	1.72, 1.34
8	2.68	2.17	2.23	2.04
9	—	3.37	3.51	2.71
10	3.08	1.96	1.94	2.00
11	3.82	3.74	3.56	3.79
12	—	—	—	—
13	5.03	4.89	5.05	4.85
14	1.91, 1.48	1.92, 1.49	1.91, 1.47	1.91, 1.48
15	0.84	0.89	0.84	0.90
16	1.18	1.20	1.20	1.20
17	1.10	1.09	1.11	1.11
18	1.46	1.26	1.32	1.22
19	1.16	1.07	0.96	1.15
20	1.14	1.17	1.15	1.13
21	1.12	1.11	1.13	1.10
22	—	—	—	—
23	—	—	1.45	—
24	—	—	1.45	—
1''	4.88	4.97	4.99	5.05
2''	2.35, 1.56	2.37, 1.59	2.36, 1.60	2.40, 1.60
3''	—	—	—	—
4''	3.00	3.03	3.04	3.05
5''	3.99	4.03	4.04	4.00
6''	1.27	1.31	1.32	1.29
7''	1.23	1.25	1.25	1.25
8''	3.31	3.31	3.33	3.35
1'	4.40	4.53	4.48	4.60
2'	3.21	3.29	3.27	3.28
3'	2.43	2.53	2.49	2.48
4'	1.67, 1.22	1.68, 1.26	1.69, 1.27	1.67, 1.25
5'	3.48	3.57	3.51	3.57
6'	1.22	1.23	1.24	1.23
7', 8'	2.29	2.31	2.32	2.30

## Results and Discussion

*Analysis of the  $^1\text{H}$  and  $^{13}\text{C}$  N.m.r. Spectra of (2), (3), and (4).*—The complex and overlapped 400 MHz  $^1\text{H}$  n.m.r. spectra of compounds (2), (3), and (4) in  $\text{CDCl}_3$  were solved using 2D  $^1\text{H}$  COSY-45 n.m.r. experiments, as done previously for (1).<sup>7</sup> The assignment of all the  $^1\text{H}$  n.m.r. spectra is unambiguous and complete, except for some of the hydroxy protons. As an example, Figure 1 shows a contour plot of the high-field region of the 400 MHz 2D  $^1\text{H}$  COSY-45<sup>8</sup> n.m.r. spectrum of (4) in  $\text{CDCl}_3$ , beneath the corresponding one-dimensional (1D) spectrum. The multitude of off-diagonal cross peaks established the connectivities between all the pairs of mutually coupled protons. There are some notable long-range connectivities e.g. 12-OH, Me-21 and 2''ax, Me-7''. The arrows on some of the cross peaks in the region above the diagonal serve to indicate their slopes. The relative signs of coupling constants in certain spin-systems can be obtained by inspection of the cross peak slope and this is useful in distinguishing between *geminal* ( $^2J < 0$ ) and *vicinal* ( $^3J > 0$ , generally) couplings.<sup>1,8</sup>

Having established unambiguous assignments of the  $^1\text{H}$  n.m.r. spectra, 2D proton, carbon-13 chemical-shift correlation experiments were used in order to obtain unambiguous assignments of the  $^{13}\text{C}$  n.m.r. spectra of (2), (3), and (4). An expansion of the 2D  $^1\text{H}$ ,  $^{13}\text{C}$  COSY n.m.r. spectrum<sup>9–11</sup> of (3)

**Table 2.**  $^{13}\text{C}$  N.m.r. chemical shifts ( $\delta_{\text{C}}$  in p.p.m.) for (1)–(4) in  $\text{CDCl}_3$ – $\text{Me}_4\text{Si}$ 

Carbon	(1) <sup>7</sup>	(2)	(3)	(4)
1	176.3	177.0	175.4	177.0
2	45.0	45.7	44.9	44.4
3	80.3	79.3	79.9	78.2
4	39.5	41.9	40.2	42.6 <sup>a</sup>
5	84.0	84.6	84.2	83.2
6	74.8	75.0	73.9	75.5
7	38.5	37.1	35.1	37.8
8	44.9	34.2	32.8	33.8
9	221.9	83.2	80.4	63.5
10	38.1	32.0	30.3	31.0
11	68.8	70.9	69.3	70.2
12	74.5	74.5	73.9	74.1
13	77.1	77.7	76.3	77.4
14	21.2	21.8	21.4	22.0
15	10.7	11.2	10.6	11.4
16	15.9	14.9	16.1	13.7
17	9.2	9.5	9.5	9.4
18	26.4	25.3	26.6	24.6 <sup>a</sup>
19	18.4	20.1	19.6	20.3
20	12.0	15.1	16.4	14.6
21	16.2	16.6	15.7	16.2
22	—	—	101.8	—
23	—	—	28.0	—
24	—	—	24.1	—
1''	96.5	96.5	96.1	95.4
2''	35.0	34.9	35.1	34.9
3''	72.7	72.7	72.9	72.8
4''	77.9	77.7	78.1	77.9
5''	65.7	66.2	65.6	65.8
6''	18.5	18.2	18.5	18.3
7''	21.4	21.6	21.6	21.7
8''	49.5	49.4	49.5	49.3
1'	103.3	103.4	102.9	102.4
2'	71.1	70.8	71.2	70.9
3'	65.3	65.1	65.5	65.3
4'	29.2	29.0	29.0	28.8
5'	68.8	69.3	68.8	69.3
6'	21.4	21.2	21.5	21.3
7', 8'	40.3	40.4	40.4	40.4

<sup>a</sup> Indicates broad resonance.

**Table 3.** Vicinal proton-proton coupling constants ( $^3J$  in Hz) for (1)–(4) in  $\text{CDCl}_3$ – $\text{Me}_4\text{Si}$ 

Coupling	(1) <sup>7</sup>	(2)	(3)	(4)
16, 2	7.5	7.0	7.1	7.1
2, 3	9.4	6.6	9.0	4.6
3, 4	1.5	2.7	1.5	2.1
4, 5	7.7	5.8	7.3	6.2
4, 17	7.4	7.2	7.5	7.2
7a, 8	11.7	~6.4	8.4	~4.6
7e, 8	~2.5	~6.8	~3–4	~8.6
8, 19	7.1	7.0	7.3	7.0
8, 9	—	5.5	3.0	6.6
9, 10	—	1.7	3.0	1.7
10, 11	1.3	1.6	2.4	1.1
10, 20	6.9	7.0	7.0	7.0
13, 14e	2.4	2.6	2.5	3.1
13, 14a	11.0	9.9	11.2	9.3
14, 15	7.4	7.3	7.4	7.5

in  $\text{CDCl}_3$  is shown in Figure 2(a) as a contour plot. Cross peaks are observed at locations  $\delta_{\text{H}_i}$ ,  $\delta_{\text{C}_i}$  where  $\text{H}_i$  and  $\text{C}_i$  are directly bonded proton and carbon-13 nuclei. Since the assignment of the  $^1\text{H}$  n.m.r. spectrum was complete, this 2D spectrum gave a

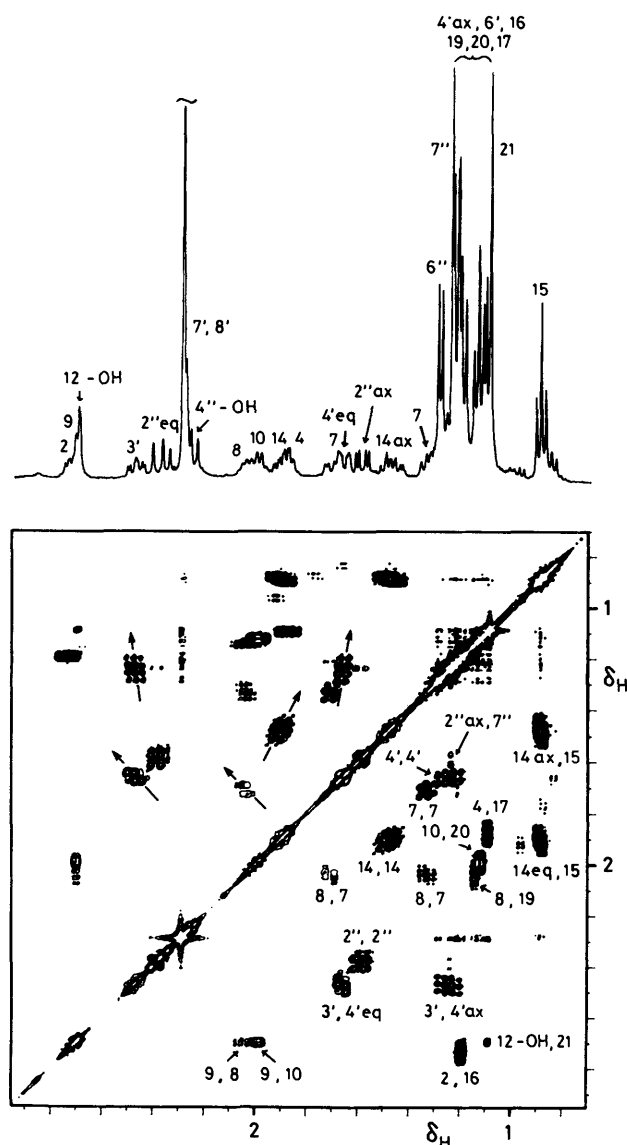


Figure 1. Contour plot of the high-field region of the 400 MHz 2D  $^1\text{H}$  COSY-45 n.m.r. spectrum of (4) in  $\text{CDCl}_3\text{-Me}_4\text{Si}$ , underneath the corresponding region of the 1D  $^1\text{H}$  n.m.r. spectrum. The arrows on some of the cross peaks serve merely to indicate their slope (see text). All cross peaks are labelled with the numbering of the proton-proton pair whose mutual  $J$ -coupling gave rise to the cross peaks

complete and unambiguous analysis of all the protonated carbons of (3), including all the methyl carbons. The same procedure was followed for (2) and (4). In the case of (3) the quaternary carbon assignments were made by use of a 2D  $^1\text{H}$ ,  $^{13}\text{C}$  COLOC experiment.<sup>12</sup> This experiment effects  $^1\text{H}$ ,  $^{13}\text{C}$  chemical-shift correlation via  $^2J_{\text{H,C}}$  and  $^3J_{\text{H,C}}$ , thus allowing the unambiguous assignment of the quaternary carbons. Figure 2(b) shows a contour plot of the 2D  $^1\text{H}$ ,  $^{13}\text{C}$  COLOC n.m.r. spectrum of (3) in  $\text{CDCl}_3$  over the same region as the 2D  $^1\text{H}$ ,  $^{13}\text{C}$  COSY spectrum in Figure 2(a). In addition to solving the quaternary carbon assignments, the mass of correlations found involving protonated carbons allowed the assignments made in the 2D  $^1\text{H}$ ,  $^{13}\text{C}$  COSY spectrum to be checked.

*The Conformational Analysis of (9S)-9-Hydroxy-9-deoxyerythromycin A (2).*—(i) *General conformational features.* The  $^3J_{\text{HH}}$  values of the sugar ring protons indicated that both the

cladinose and desosamine sugar rings were in the same chair conformations as in (1).<sup>1</sup>

The pattern of  $^1\text{H}$  n.O.e.s<sup>13</sup> involving the sugar protons further indicated that the orientations of the sugar rings with respect to one another and with respect to the lactone ring were very similar to those found in (1).<sup>1,2</sup> However an inspection of the matrix of  $^1\text{H}$  n.O.e.s of (2) in  $\text{CDCl}_3$  (Table 4) showed that whilst (2) exhibited all but three of the intra-lactone n.O.e.s of (1), eleven new intra-lactone n.O.e.s were found, not including those involving 9-H.<sup>2</sup> The n.O.e. from 11-H to 3-H i.e. n.O.e.[11]3 was larger than n.O.e.[11]4 in (2) whereas for (1) n.O.e.[11]3 was barely detectable and n.O.e.[11]4 was  $\sim 4\%$ .<sup>1,2</sup> Other striking differences between the behaviour of (1) and (2) were observed upon irradiation of 8-H (Figure 3). The new n.O.e.s from 8-H to 3-H and 5-H in (2) were completely absent in (1). It was concluded that (2) could occupy lactone ring conformations different from those of (1).<sup>2</sup>

The lactone ring  $^3J_{\text{HH}}$  values<sup>2</sup> of (2) (Table 3) were also quite different to those of (1), in support of this conclusion. When the  $^3J_{\text{HH}}$  values were remeasured in  $\text{CD}_3\text{OD}$  solution further large changes were observed e.g.  $^3J_{2,3} \sim 6.6$  ( $\text{CDCl}_3$ )  $\rightarrow$  4.5 Hz ( $\text{CD}_3\text{OD}$ ). These  $^3J_{\text{HH}}$  changes were indicative of fast conformational averaging between 2 or more lactone ring conformations, the proportions of each conformation changing between the different solvents.

N.O.e. kinetics experiments showed a similar (medium) rate of build-up for n.O.e.[11]3, n.O.e.[11]4, and n.O.e.[11]8 in both  $\text{CDCl}_3$  and  $\text{CD}_3\text{OD}$  solvents (Figure 4). In conjunction with the  $^3J_{\text{HH}}$  data these results led to the conclusion that the lactone ring of (2) was in fast equilibrium between two or more conformations. One conformation was very similar to the crystalline-state conformation<sup>14</sup> of the hydroiodide dihydrate of (1) thus giving rise to all the n.O.e.s characteristic of this conformation.<sup>1,2</sup> The other conformation(s) has  $r_{4,11} > 3 \text{ \AA}$  but  $r_{3,11}$ ,  $r_{3,8}$  and  $r_{8,11}$  all  $< 3 \text{ \AA}$  thus giving rise to the new n.O.e.s observed for (2). This conclusion is novel since previous n.m.r. work<sup>15-25</sup> indicates that all erythromycins are expected to adopt an alternate diamond-lattice conformation in solution, similar to the crystal structure of (1).<sup>14</sup>

(ii) *Crystalline-state models for the new ring conformations.*

A search was made of the crystal structures of related erythromycins in order to find models for the new lactone ring conformation(s) exhibited by (2). A suitable model was found in the crystal structure of (5)<sup>26</sup> (shown in Figure 5 without its long ether side chain for clarity). Comparison with the crystal structure of the hydroiodide dihydrate of (1) (Figure 6) shows many differences. Rotation, principally about the C-2-C-3 and C-5-C-6 bonds, has caused the C-3 to C-5 portion of the macrocyclic ring to 'fold inwards' such that 3-H becomes much closer to 11-H (2.2 vs. 3.7  $\text{\AA}$ ). In addition a reorganisation of the C-6-C-9 portion of the ring has caused 8-H to fold into the ring thereby coming closer to 3-H (2.2 vs. 5.9  $\text{\AA}$ ), 5-H (2.3 vs. 4.9  $\text{\AA}$ ), and 11-H (2.5 vs. 4.2  $\text{\AA}$ ). However, the C-10-C-13 portion of the macrocyclic ring remains in a similar conformation. Furthermore, the similarity of  $\phi_{\text{C}_3\text{C}_4}$  and  $\phi_{\text{C}_4\text{C}_5}$  in the two crystal structures means that the orientations of the sugar rings with respect to one another remain the same, even though in (5) they are now folded-in towards the C-9-C-12 side of the ring. Table 5 compares the lactone ring torsion angles in the crystal structure of (1) and (5). Table 6 gives the spatial proximity map<sup>1</sup> for pairs of protons less than 3  $\text{\AA}$  apart in the crystal structure of (5). For conciseness, the crystalline-state conformations of erythromycin A hydroiodide dihydrate and (5) will now be referred to as A and B respectively.

(iii) *Comparison of the solution-state conformations of (2) with the crystalline-state conformations A and B.* The matrix of n.O.e.s observed for (2) in  $\text{CDCl}_3$  (Table 4) is equivalent to a proton-proton spatial proximity map of the solution state. Comparison

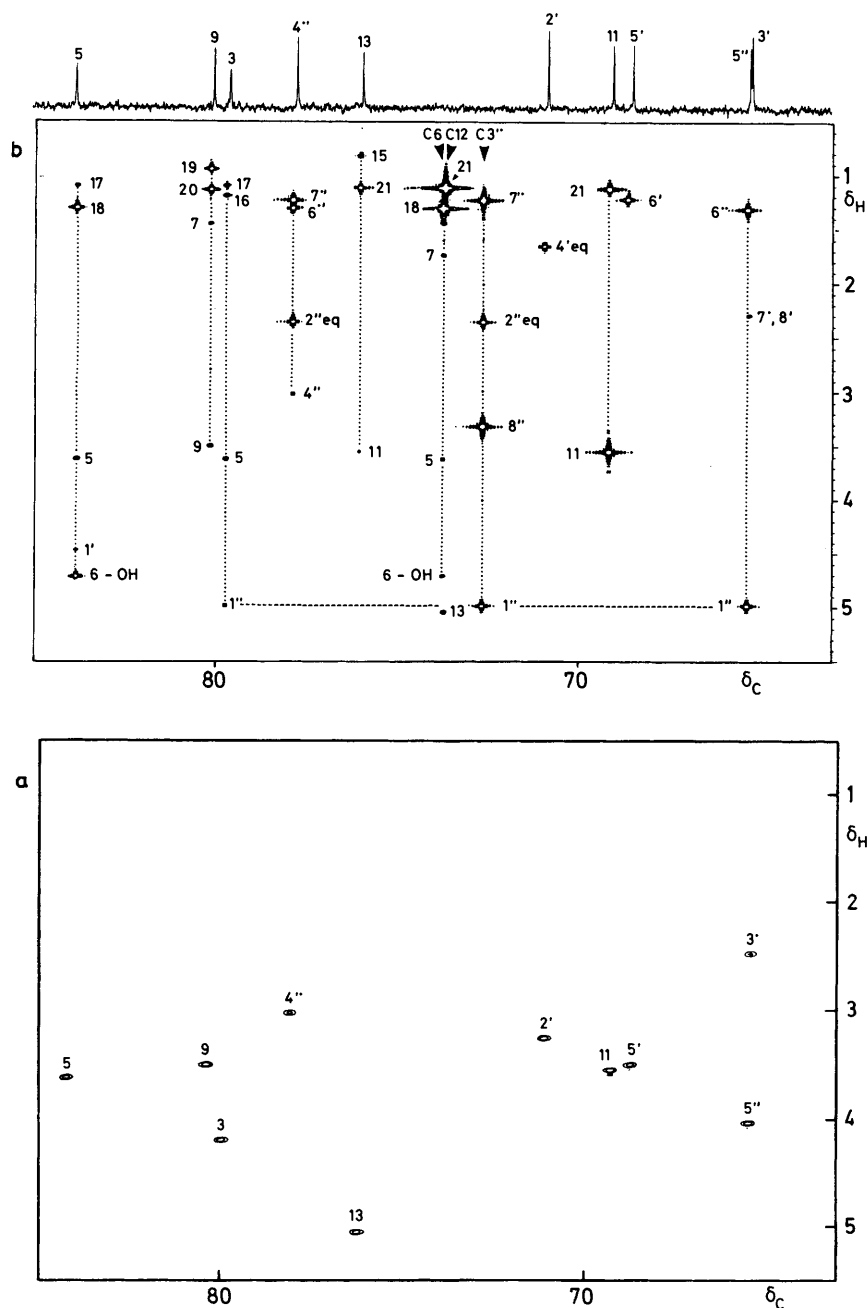


**Figure 2(a).** Contour plot of an expansion of the 2D  $^1\text{H}$ ,  $^{13}\text{C}$  COSY n.m.r. spectrum of (3) in  $\text{CDCl}_3\text{-Me}_4\text{Si}$ . Each cross peak is a singlet due to broadband  $^1\text{H}$  decoupling in both dimensions. **Figure 2(b).** Contour plot of the same expansion of the 2D  $^1\text{H}$ ,  $^{13}\text{C}$  COLOC n.m.r. spectrum of (3) in  $\text{CDCl}_3\text{-Me}_4\text{Si}$  underneath the corresponding region of the 1D distortionless enhancement by polarisation transfer (DEPT)-90  $^{13}\text{C}$  n.m.r. spectrum. The vertical dotted lines (...) link all the cross peaks due to the correlation of several proton resonances with one carbon-13 resonance. The horizontal dashed line(---) links all the  $^{13}\text{C}$  resonances which have a correlation with 1'-H. Note that the quaternary carbon resonances are suppressed in the DEPT spectrum

of this map with the spatial proximity maps for **A**<sup>1</sup> and **B** (Table 6) showed that features of both crystalline-state conformations were exhibited by (2) in the solution state.

Conformation **B** has a close approach of 3-H and 11-H, thus explaining the very large value of n.O.e.[11]3 in (2) relative to (1) (~1.9% vs. 0.2%).<sup>1,2</sup> Conformation **B** also has Me-18 folded down and under the lactone ring such that  $r_{18,4} \sim 2.0$  Å min (cf. 4.3 Å in **A**) but  $r_{18,5}$  and  $r_{18,8} > 3.5$  Å in **B**, compared with 1.9 Å min and 2.2 Å min respectively in **A**. Irradiation of Me-18 gave medium-sized n.O.e.s to 4-H, 5-H, and 8-H thus confirming the contribution of conformations like **B** to a blend including **A**.

The remarkable observation of n.O.e.s from 8-H to 3-H, 5-H, and 11-H (Figure 3) can only be explained by a substantial contribution of conformation **B**, where 8-H is oriented into the lactone ring (see Figure 5). On the other hand, the medium-sized n.O.e.[8]9 (Figure 3) can only be explained by a substantial contribution from a lactone ring conformation equivalent to **A** (but with an  $sp^3$  C-9).

In summary the  $^1\text{H}$  n.O.e. data indicated that the minimum representation of the solution-state equilibrium of (2) was  $\text{A} \rightleftharpoons \text{B}$ .

The contribution of conformations like **B** to the conform-



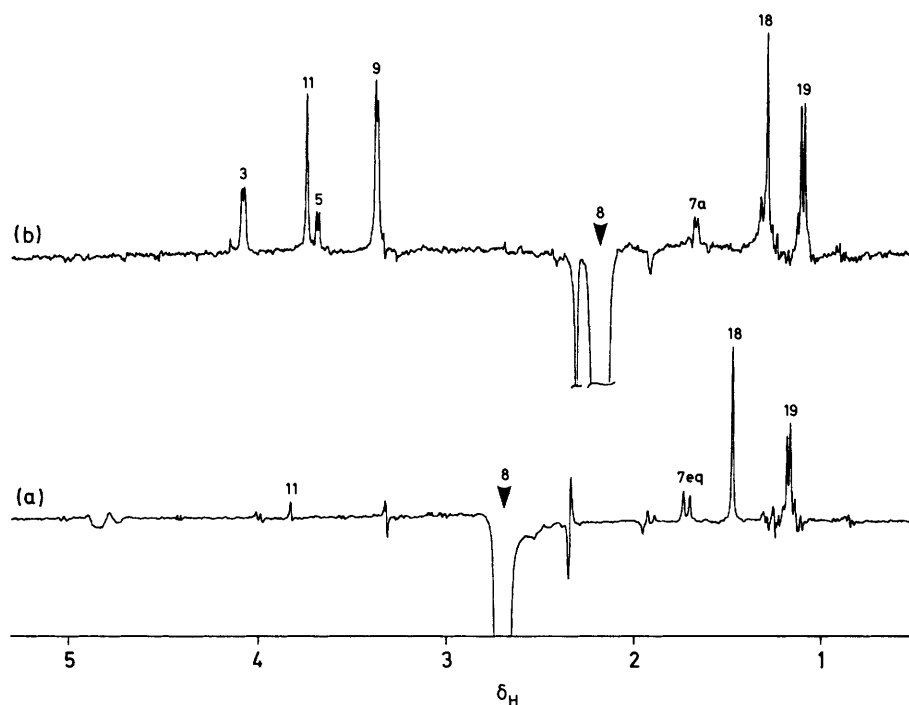


Figure 3. Two 400 MHz  $^1\text{H}$  n.o.e. difference spectra due to the irradiation of 8-H in (a) (1) and (b) (2)

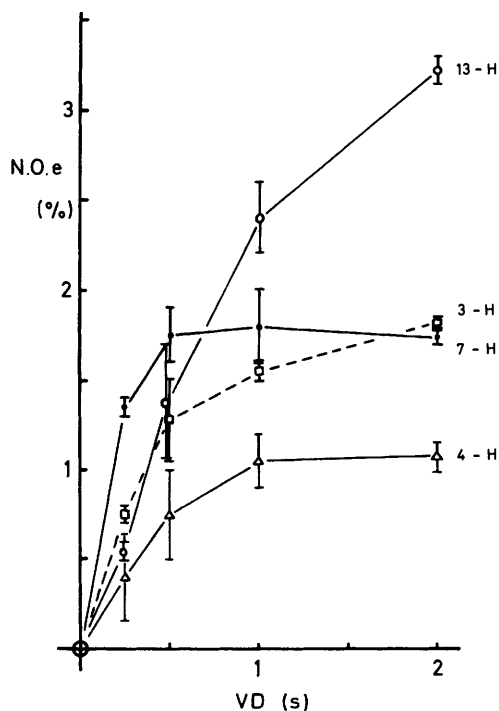


Figure 4. A graph of n.o.e. in % vs. irradiation time VD in s for the irradiation of 11-H in (2) dissolved in  $\text{CD}_3\text{OD}$ . The data for n.o.e. [11]8 are omitted for clarity but displayed a medium rate of build-up—similar to n.o.e. [11]3 and n.o.e. [11]4. The points and error bars represent the averages and ranges respectively of data from two experiments run under the same conditions

ational blend of (2) in solution was further tested using  $^{13}\text{C}$  n.m.r. relaxation time experiments.<sup>1,27</sup> Conformation A is characterised by a very high energy barrier to the rotation of Me-16.<sup>1,2</sup> In B the inward folding of the C-3—C-5 portion of

Table 5. Lactone ring torsion angles ( $\phi$  in  $^\circ$ ) for the crystal structures of (1) and (5)

Torsion angle $\phi$	(1)	(5)
O1—C1—C2—C3	115.9	94.4 <sup>a</sup>
C1—C2—C3—C4	-61.2	-129.6 <sup>a</sup>
C2—C3—C4—C5	164.8	172.8
C3—C4—C5—C6	-116.1	-116.9
C4—C5—C6—C7	-68.5	67.6 <sup>a</sup>
C5—C6—C7—C8	175.0	55.5 <sup>a</sup>
C6—C7—C8—C9	-77.0	177.4 <sup>a</sup>
C7—C8—C9—C10	-60.8	34.5 <sup>a,b</sup>
C8—C9—C10—C11	122.0	70.3 <sup>a,b</sup>
C9—C10—C11—C12	-173.3	-156.0
C10—C11—C12—C13	167.8	-173.6
C11—C12—C13—C14	165.1	164.5
C12—C13—O1—C1	107.3	156.0 <sup>a</sup>
C13—O1—C1—C2	171.3	-173.6

<sup>a</sup>  $\Rightarrow \phi$  (1) different to  $\phi$  (5) by  $> 20^\circ$ . <sup>b</sup> n.b. comparing  $sp^2$  C-9 in (1) with  $sp^3$  C-9 in (5).

the lactone ring removes the steric hindrance to the rotation of Me-16 and the calculated rotational energy barrier drops by a factor of 5 (Table 7). In (1) the adoption of a solution-state conformation very similar to A gave rise to a very low  $^{13}\text{C}$   $NT_1$  value<sup>28,29</sup> for Me-16 relative to other methyl groups e.g. Me-17.<sup>1,2</sup> However, it can be clearly seen (Figure 7 and Table 7) that the  $^{13}\text{C}$   $NT_1$  values of Me-16 and Me-17 in (2) are approximately equal. This result confirmed that in solution (2) adopted conformations like B (as well as A) which have reduced energy barriers to the rotation of Me-16. The corresponding  $^1\text{H}$   $T_1$  data was in agreement with this conclusion (Table 7). The  $^{13}\text{C}$   $NT_1$  data also indicated less preferential mobility of the desosamine sugar relative to the cladinose sugar than in (1).<sup>1</sup> The averaged  $^{13}\text{C}$   $NT_1$  values for the protonated carbons of the lactone, cladinose and desosamine rings were  $0.45 \pm 0.03$ ,  $0.48 \pm 0.03$ , and  $0.51 \pm 0.01$  s respectively.

(iv) Summary. (9S)-9-Hydroxy-9-deoxyerythromycin A (2)

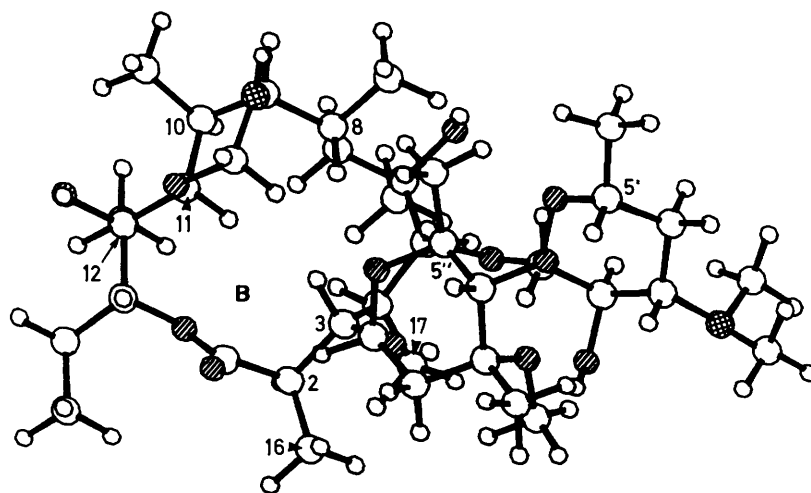


Figure 5. Crystal structure of (9*S*)-9-*N*,11-*O*-[2-(2-methoxyethoxy)ethylidene]erythromyclamine A (5), shown without the long ether side chain for clarity. Oxygen atoms are shaded and nitrogen atoms cross-hatched

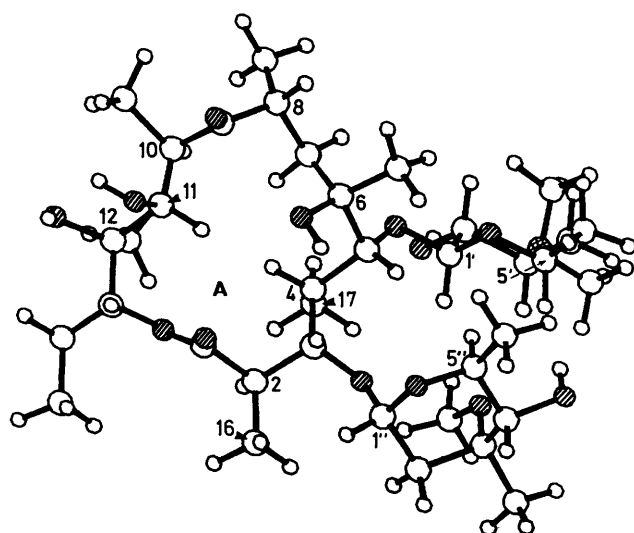


Figure 6. Crystal structure of erythromycin A hydroiodide dihydrate. Oxygen atoms are shaded and the nitrogen atom cross-hatched

exists in  $\text{CDCl}_3$  and  $\text{CD}_3\text{OD}$  solution as a mixture of lactone ring conformers in fast exchange. A minimal description of this mixture would involve an equilibrium between lactone rings in the model conformations A and B. In reality the equilibrium is probably between two types of ring conformations; those with a 'folded-out' C-3—C-5 region (A) and those with a 'folded-in' C-3—C-5 region (B). Each type of ring conformation is in turn unstable in the C-6—C-9 region. It was of interest to note that the *in vitro* antibacterial activity of (2) against a range of representative organisms was 16—32 times lower than (1).<sup>30</sup>

*The Conformational Analysis of (9S)-9,11-O-Isopropylidene-9-deoxyerythromycin A (3).*—The  $^3J_{\text{H,H}}$  values of the sugar ring protons indicated that both the cladinose and desosamine sugar rings were in the same chair conformations as (1).<sup>1</sup>

The pattern of  $^1\text{H}$  n.o.e.s (Table 8) involving the sugar protons further indicated that the orientations of the sugar rings with respect to one another and with respect to the lactone ring were indistinguishable from those found for (1) in  $\text{CDCl}_3$  solution.<sup>1</sup>

The  $^3J_{\text{H,H}}$  values of the lactone ring protons (Table 3) were similar to those found in (1) but the values of  $^3J_{7_{\text{ax}},8} \sim 8.4$  and

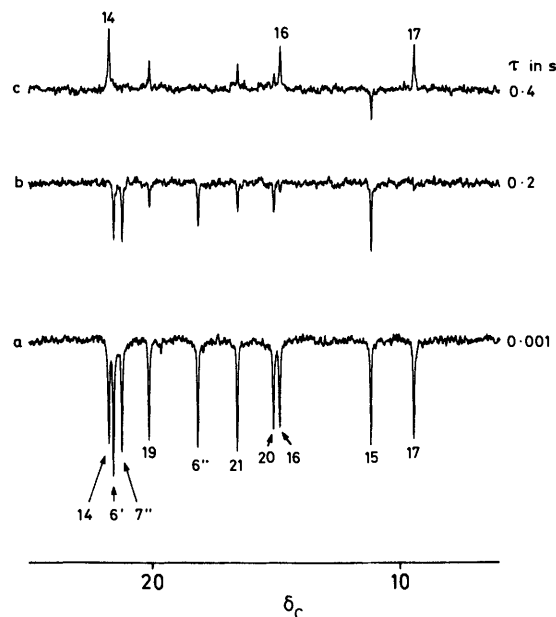


Figure 7. Three partially relaxed 100 MHz  $^{13}\text{C}$  n.m.r. spectra of (2) in  $\text{CDCl}_3$  taken from an inversion-recovery  $T_1$  experiment with variable delays  $\tau$  (in between the  $180^\circ$  and  $90^\circ$  pulses) of 0.001, 0.2, and 0.4 s. Note the similar relaxation rates for Me-16 and Me-17

$^3J_{7_{\text{eq}},8} \sim 3\text{--}4$  Hz were indicative of some degree of conformational freedom in the C-6 to C-9 region. Inspection of the matrix of  $^1\text{H}$  n.o.e.s for (3) (Table 8) showed that the pattern of n.o.e.s involving the lactone protons was very similar to that found in (1) (neglecting interactions involving 9-H).<sup>1</sup> The only exceptions to this were the small n.o.e.[21]13 and n.o.e.[6'']1' which had not been observed for (1). The former n.o.e. was probably a long-range effect in A ( $r_{\text{min}} \sim 3.4 \text{ \AA}$ ) whilst the latter n.o.e. was probably indicative of (3) populating a conformation with a sugar-sugar interaction different to those found in A or B. As in (1) there was a minor population of another lactone ring conformation different to A which gave rise to very small values of n.o.e.[3]11 ( $\sim 0.1\%$ ) and n.o.e.[11]3 (0.3%). In view of the results obtained on (2), this minor conformation of (1) and (3) was probably a 'folded-in' conformation like B.

In summary, the  $^3J_{\text{H,H}}$  and  $^1\text{H}$  n.o.e. data indicated that the dominant solution conformation of (3) was A with a minor





**Table 7.** Calculated rotational energy barriers (crystal structures) and experimental  $^{13}\text{C}$  and  $^1\text{H}$  n.m.r. relaxation times ( $\text{CDCl}_3$  solution) for the methyl groups in (1)–(5)

Methyl	$\Delta E^a$ (kcal mol $^{-1}$ )		$^{13}\text{C } NT_1$ and ( $^1\text{H } T_1$ ) (s) <sup>b</sup>			
	(1)	(5)	(1)	(2)	(3)	(4)
15	A	A	3.0 (0.52)	3.6 (0.59)	— (0.53)	3–4 (0.66)
16	F	B	0.78 (0.20)	1.25 (0.29)	0.9 (0.20)	1.3 (0.31)
17	C	D	1.80 (0.33)	1.23 (0.26)	2.2 (0.33)	1.2 (0.29)
18	C	B	1.9 (0.30)	1.77 (0.33)	2.6 (0.35)	1.58 (0.33)
19	B	D	1.56 (0.29)	1.47 (0.29)	— (0.26)	1.7 (0.33)
20	B	B	2.1 (0.38)	1.76 (0.35)	2.6 (0.33)	1.5 (0.33)
21	C	B	1.48 (0.28)	1.61 (0.31)	2.2 (0.33)	1.7 (0.33)
8''	A	A	3.4 (0.59)	4–5 (0.62)	>3 (0.63)	>3 (0.59)

<sup>a</sup> Theoretical calculations based upon the crystal structures of (1) and (5). The results are given in terms of energy barrier ranges—A(0–2), B(2–5), C(5–10), D(10–15), E(15–20), and F(20–30 kcal mol $^{-1}$ ). These ranges must be regarded as very approximate. The hard-sphere calculations employed did not allow the molecule to relax as the methyl group was rotated—hence the calculated energy barriers will be overestimated. <sup>b</sup> Experimental results in  $\text{CDCl}_3$  solution at ambient temperature;  $T_1$  = spin-lattice relaxation time;  $N = 3$ , the number of protons on each carbon. The average error of the  $^1\text{H } T_1$  determinations (null-point method) was estimated to be  $\pm 0.03$  s for all compounds. The  $^{13}\text{C } NT_1$  errors for (1) are given in reference 1. The  $^{13}\text{C } NT_1$  values for (2) are the average of two determinations with  $\sigma = 0.06$  and  $\sigma = 0.03$  (averages). The  $^{13}\text{C } NT_1$  values for (3) and (4) are the result of single determinations with  $\sigma = 0.08$  (average) and  $\sigma = 0.10$  s (average) respectively.

contribution from B and that the C-6–C-9 region was possibly less stable than in (1).

This conclusion was tested using  $^{13}\text{C}$  n.m.r. relaxation measurements. The  $^{13}\text{C } NT_1$  value of Me-16 was found to be less than half that of Me-17 (Table 7) as expected<sup>28,29</sup> on the basis of the domination of A. The corresponding  $^1\text{H } T_1$  data was in agreement with this conclusion and showed that the  $T_1$  of Me-16 was much less than that of Me-17 (Figure 8, Table 7). The *in vitro* antibacterial activity of (3) against a range of representative organisms was only  $\sim 1$ –4 times lower than that of (1).<sup>30</sup> The possibility of an association between antibacterial activity and conformational stability (dominance of A) was noted.

*The Conformational Analysis of (9S)-Erythromyclamine A (4).*—The  $^3J_{\text{H,H}}$  values of the sugar ring protons indicated that both the cladinose and desosamine sugar rings of (4) were in the same chair conformations as (1).<sup>1</sup>

The pattern of  $^1\text{H}$  n.O.e.s involving the sugar protons (Table 9) indicated that their mutual orientation and their orientations with respect to the lactone ring were very similar to those found for (1).<sup>1</sup> This is well illustrated in Figure 9 which shows a contour plot of an expansion of the phase-sensitive 2D NOESY  $^1\text{H}$  n.m.r. spectrum of (4) in  $\text{CDCl}_3$ . The inter-sugar and sugar–lactone n.O.e.s such as n.O.e.[1'']5'', n.O.e.[1']5, n.O.e.[1'']3, n.O.e.[5'']5, and the weak n.O.e.[5'']5' are the same interactions previously observed in (1).<sup>1</sup>

The  $^3J_{\text{H,H}}$  values of the lactone ring protons (Table 3) were indicative of fast conformational averaging between two or

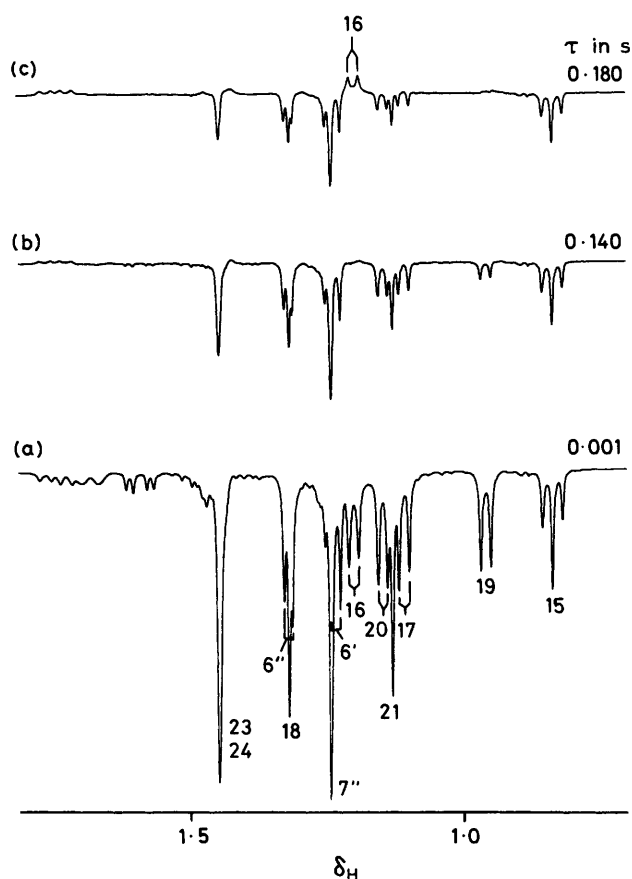


**Figure 8.** Three partially relaxed 400 MHz  $^1\text{H}$  n.m.r. spectra of (3) in  $\text{CDCl}_3$  taken from an inversion-recovery  $T_1$  experiment with variable delays  $\tau$  (in between the  $180^\circ$  and  $90^\circ$  pulses) of 0.001, 0.140, and 0.180s. Note the very fast relaxation rate of Me-16

more lactone ring conformations, as in (2). The pattern of lactone ring n.O.e.s (Table 9, Figure 10) was similar to that of (2) (Table 1). The observation of n.O.e.[11]3 ( $\sim 2.5\%$ ) being twice as large as n.O.e.[11]4 ( $\sim 1.2\%$ ) indicated that in (4) the equilibrium was more biased towards B than A. The observation of n.O.e.s from 8-H to 3-H, 5-H, and 11-H confirmed the contribution of conformations like B (Figure 6) and the observation of n.O.e.[8]18 and n.O.e.[11]4 confirmed the contribution of conformations like A to the conformational equilibrium (Figure 10). However, the observation of n.O.e.s from 11-H to both 7-H protons indicated that the C-6–C-9 region of the molecule was conformationally flexible, as was found for (2).

As for (2) the  $^{13}\text{C } NT_1$  values for Me-16 and Me-17 were approximately equal (Table 5) indicative of the contribution of 'folded-in' lactone ring conformations without restricted rotation of Me-16. The  $^{13}\text{C } NT_1$  data also indicated less preferential mobility of the desosamine sugar relative to the cladinose sugar than in (1), as was found for (2). The averaged  $^{13}\text{C } NT_1$  values of protonated carbons of the lactone, cladinose, and desosamine rings were  $0.43 \pm 0.02$ ,  $0.46 \pm 0.04$ , and  $0.49 \pm 0.02$  s respectively.

In summary, the n.m.r. data indicated that in  $\text{CDCl}_3$  solution (4) was in fast conformational equilibrium between conformations with 'folded-out' (A) and 'folded-in' (B) C-3 to C-5 lactone ring regions. This conformational equilibrium was very similar to that found for (2) but was probably more biased towards the 'folded-in' conformations. The *in vitro* antibacterial activity of (4) against a range of representative organisms is in





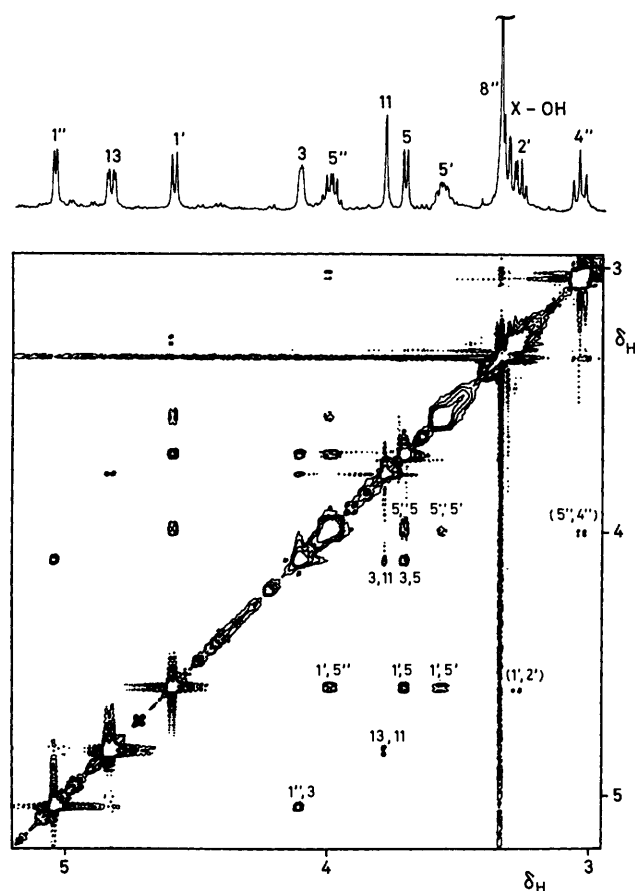


Figure 9. Contour plot of the low-field region of the 400 MHz 2D phase-sensitive  $^1\text{H}$  NOESY spectrum of (4) in  $\text{CDCl}_3$  underneath the corresponding 1D  $^1\text{H}$  n.m.r. spectrum. Positive and negative levels are plotted without distinction

the range 0.5–2 times lower than (1) *i.e.* it is quite active. Thus, the simple correlation between conformational stability in  $\text{CDCl}_3$  solution and *in vitro* antibacterial activity, which had been emerging in the series of compounds (1)–(3), was unfounded.

### Conclusions

The combined use of  $^1\text{H}$  n.m.r. n.O.e. experiments and  $^{13}\text{C}$   $T_1$  experiments has been shown to be a very powerful tool with which to probe the solution-state conformations of a series of erythromycin antibiotics. The experiments have conclusively shown that some erythromycin A derivatives exist in solution with their lactone rings in fast exchange between conformations which have been characterised as 'folded-in' or 'folded-out' in the C-3–C-5 region.

Molecular modelling techniques were used to compare the actual solution-state n.O.e. and  $T_1$  n.m.r. data with those expected for crystalline-state models of the two lactone ring conformations.

These findings are novel and go against previous literature reports which suggest conformational stability in the C-3–C-5 region unless a drastic chemical modification is made in that region.

No simple correlation between solution-state conformational behaviour and antibacterial activity was found for compounds (1)–(4).

### Experimental

The 1D  $^1\text{H}$  and  $^{13}\text{C}$  n.m.r. experiments and the 2D  $^1\text{H}$  COSY-45, 2D  $^1\text{H}$  NOESY, and 2D  $^1\text{H}$ ,  $^{13}\text{C}$  COSY experiments were performed as described previously<sup>1,7</sup> on a Bruker AM400 n.m.r. spectrometer using a 5 mm  $^1\text{H}/^{13}\text{C}$  dual probe at ambient temperature and sample concentrations of  $\sim 20 \text{ mg ml}^{-1}$  in  $\text{CDCl}_3$ . However, the 100 MHz  $^{13}\text{C}$   $T_1$  experiments were conducted<sup>7</sup> in the 10 mm  $^{13}\text{C}$  probe of the same instrument at  $\sim 300 \text{ K}$ . Some experiments were conducted under conditions of

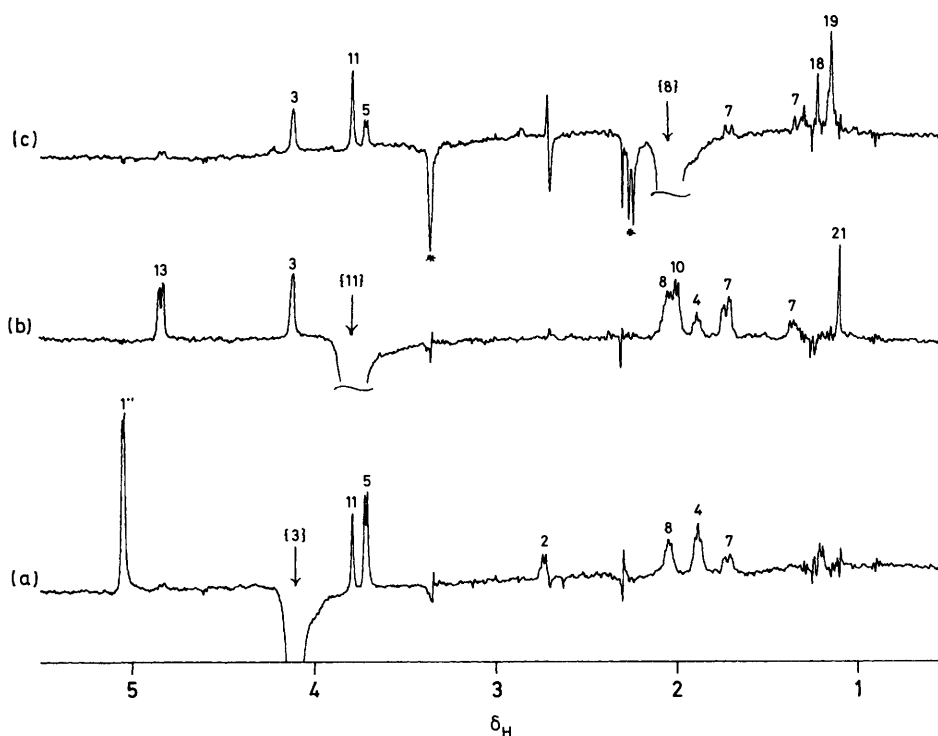


Figure 10. Three 400 MHz  $^1\text{H}$  n.O.e. difference spectra of (4) in  $\text{CDCl}_3$  obtained by the irradiation of (a) 3-H, (b) 11-H, and (c) 8-H

D<sub>2</sub>O exchange and/or at slightly elevated temperatures (~300–310 K) in order to improve resolution. The 2D <sup>1</sup>H, <sup>13</sup>C COLOC experiment was conducted using the standard Bruker program. F.I.D.s were acquired (128 scans, four dummy scans) over 20 kHz, into an 8 K data block for 256 incremented values of the evolution time. The polarisation delay D2 was 0.0531 s and the refocusing delay D3 was 0.0266 s. The raw data were zero-filled to an 8 K × 1 K matrix and processed with a 2 Hz line-broadening function in both dimensions, prior to double Fourier transformation.

### Acknowledgements

Our thanks are due to Dr. E. Hunt and Mr. A. Zomaya for the supply of purified compounds, to Drs. E. Hunt, P. Finn, D. Neuhaus, and J. M. Wilson for helpful discussions, and to Miss A. Bentley for careful typing.

### References

- 1 J. R. Everett and J. W. Tyler, *J. Chem. Soc., Perkin Trans. 2*, 1987, 1659.
- 2 J. R. Everett and J. W. Tyler, *J. Chem. Soc., Chem. Commun.*, 1987, 815.
- 3 M. V. Sigal, P. F. Wiley, K. Gerzon, E. H. Flynn, U. C. Quarck, and O. Weaver, *J. Am. Chem. Soc.*, 1956, **78**, 388.
- 4 T. Glabski, H. Bojarska-Dahlig, and W. Slawinski, *Roczniki Chemii*, 1976, **50**, 1281.
- 5 E.P. Appl. 184921A (Beecham), 1986.
- 6 G. H. Timms and E. Wildsmith, *Tetrahedron Lett.*, 1971, 195.
- 7 J. R. Everett and J. W. Tyler, *J. Chem. Soc., Perkin Trans. 1*, 1985, 2599.
- 8 A. Bax, 'Two-dimensional Nuclear Magnetic Resonance in Liquids,' D. Reidel, Dordrecht, 1984.
- 9 A. Bax, *J. Magn. Reson.*, 1983, **53**, 517.
- 10 V. Rutar, *J. Magn. Reson.*, 1984, **58**, 306.
- 11 J. A. Wilde and P. H. Bolton, *J. Magn. Reson.*, 1984, **59**, 343.
- 12 H. Kessler, C. Griesinger, and J. Lautz, *Angew. Chem., Int. Ed. Engl.*, 1984, **23**, 444.
- 13 J. H. Noggler and R. E. Schirmer, 'The Nuclear Overhauser Effect. Chemical Applications,' Academic Press, New York, 1971.
- 14 D. R. Harris, S. G. McGeachin, and H. H. Mills, *Tetrahedron Lett.*, 1965, 679.
- 15 T. J. Perun and R. S. Egan, *Tetrahedron Lett.*, 1969, 387.
- 16 L. A. Mitscher, B. J. Slater, T. J. Perun, P. H. Jones, and J. R. Martin, *Tetrahedron Lett.*, 1969, 4505.
- 17 T. J. Perun, R. S. Egan, P. H. Jones, J. R. Martin, L. A. Mitscher, and B. J. Slater, *Antimicrob. Agents Chemother.*, 1969, 116.
- 18 T. J. Perun in 'Drug Action and Drug Resistance in Bacteria 1. Macrolide Antibiotics and Lincomycin,' ed. S. Mitsushashi, University Park Press, Baltimore, 1971, p. 123.
- 19 R. S. Egan, T. J. Perun, J. R. Martin, and L. A. Mitscher, *Tetrahedron*, 1973, **29**, 2525; *J. Am. Chem. Soc.*, 1975, **97**, 4578.
- 20 R. S. Egan, Ph.D. Thesis, University of Illinois at the Medical Center, 1971.
- 21 J. G. Nourse and J. D. Roberts, *J. Am. Chem. Soc.*, 1975, **97**, 4584.
- 22 S. Ömura, A. Neszmélyi, M. Sangaré, and G. Lukacs, *Tetrahedron Lett.*, 1975, 2939.
- 23 A. Neszmélyi and H. Bojarski-Dahlig, *J. Antibiotics*, 1978, **31**, 487.
- 24 M. S. Puar and R. Brambilla, *J. Chem. Soc., Perkin Trans. 2*, 1980, 1847.
- 25 S. Ömura, 'Macrolide Antibiotics, Chemistry, Biology and Practise,' Academic Press, 1984.
- 26 P. Luger and R. Maier, *J. Cryst. Mol. Struct.*, 1979, **9**, 329.
- 27 G. C. Levy, *Acc. Chem. Res.*, 1973, **6**, 161.
- 28 W. J. Chazin and L. D. Colebrook, *Magn. Reson. Chem.*, 1985, **23**, 597.
- 29 J. Bastard, J. M. Bernassau, D. Khac Duc, M. Fetizon, and E. Lesuer, *J. Phys. Chem.*, 1986, **90**, 3936; J. M. Bernassau, M. Fetizon, I. Hanna, and J. A. Pinheiro, *ibid.*, p. 3941.
- 30 J. M. Wilson, personal communication.

Received 5th March 1987; Paper 7/411